The Raunis section, central Latvia, revisited – first luminescence results and re-evaluation of a key Baltic States stratigraphic site

Edyta Kalińska[1,2], Helena Alexanderson[3,4], Māris Krievāns[5]

[1] Nicolaus Copernicus University in Toruń, Faculty of Earth Sciences and Spatial Management, Department of Geomorphology and Quaternary Paleogeography, Lwowska 1, PL-87-100 Toruń, Poland, edyta.kalinska@umk.pl

[2] University of Tartu, Faculty of Science, Department of Geology, Ravila 14A, EE-50411, Tartu, Estonia

[3] Lund University, Department of Geology, Sölvegatan 12, SE-223 62, Lund, Sweden

[4] UiT Arctic University of Norway, Department of Geosciences, Dramsveien 201, N-9037 Tromsø, Norway

[5] University of Latvia, Faculty of Geography and Earth Sciences, Jelgavas 1, LV-1004 Riga, Latvia

Abstract

In interstadial deposits, sand interbeds gain limited consideration in comparison with organic sediments, and therefore tend to be underrepresented in palaeoenvironmental reconstructions. The Raunis site, central-eastern Latvia, is an example where organic beds have already gained some attention and been used to understand the complex interactions between advance and retreat of the Scandinavian Ice Sheet in the region. Sandy interlayers have so far not been investigated in detail and their time of deposition has also been unknown, therefore exploring these clastic-organic sediment alternation is of interest. This study provides a new set of luminescence datings along with sedimentological information from the character of individual quartz grains as detected from scanning electron microscope (SEM) analysis. Sandy interlayers are dated to between 12 ka and 122 ka. Fast component OSL signal dominates in all investigated samples, but several samples have broad and/or skewed dose distributions. Only one sample is considered reliable and provides an age

of 12.0±0.6 ka. A radiocarbon age from organic sediments in the same unit yields an age of 14,025±270 cal y BP. These two dates do not agree within 2 sigma, and this is likely related to reservoir and hard water effects of the radiocarbon sample. Sediments at the Raunis site fall into the Greenland Interstadial 1 (GI-1), but more detailed specification is not possible. The rest of the OSL ages are older than expected, likely due to incomplete bleaching during deposition. This means that stratigraphic reliability of this key site is likely hampered for further regional correlation.

Key words: clastic interbeds, optically stimulated luminescence (OSL) datings, scanning electron microscopy (SEM)

Introduction

Identification and dating of sub- and intra-till deposits that formed during interglacial or interstadial conditions can be used to infer climatic changes and glacier oscillations. Interglacial or interstadial organic sediments usually receive much attention (Battarbee 2000), since they are suitable for radiocarbon dating and for detailed microfossil and geochemistry-based environmental reconstructions. However, clastic interbeds are also important for establishing Quaternary stratigraphy and have been key components in identifying and dating ice-free periods in many areas (Houmark-Nielsen 2010; Alexanderson et al. 2014; Lunkka et al. 2015; Möller and Murray 2015). However, these sand interbeds have gained a limited attention in palaeoenvironmental studies.

At Raunis in central-eastern Latvia (Figure 1), alternating organic and clastic sediments form a nearly 3-m thick sediment succession exposed in a river cut. The organic deposits have been interpreted to represent a pre-Bølling warm interstadial, the Raunis interstadial (Bitinas 2012). This interstadial is traditionally considered as a marker in the Late Glacial interval (Pirrus and Raukas 1996; Raukas 2009), and has been used to understand the complex interactions between advance and retreat of the Scandinavian Ice Sheet (SIS), with an emphasis on the age of the oldest (=Haanja) Late Glacial Estonian end moraine zone (Kalm et al. 2011). Sediments and events from outside the

Baltic area have also been correlated with the so called Raunis Interstadial, for example in the Central Russian Upland (Rivals et al. 2018; Sycheva et al. 2016), in the Ural Mountains (Potapova 2001), the New Siberian Islands (Anisimov and Tumskoy 2002), the Caspian Sea (Oglu Aleskerov et al. 2010), the Pannonian Basin (Vandenberghe and Sidorchuk 2020), and the Black Sea (Major et al. 2002). Raunis is therefore a key section, particularly for the south-eastern Baltic region (Bitinas 2012) and a well-defined age for the sediments is of importance.

In this study, we focus on the clastic beds at Raunis for age determination and palaeoenvironmental reconstruction. The Raunis organic sediments (unit 2 in this study) have previously been subjected to numerous attempts of radiocarbon dating, giving contradictory results. We use optically stimulated luminescence (OSL) for the first time to date sandy beds that occur in this section, combined with a single new AMS radiocarbon dating of a silty organic-rich horizon that has already gained large attention (see Previous studies). We use this and existing radiocarbon dates from the Raunis section for independent comparison of OSL ages. Additionally we focus on clastic sediment properties such as the character of individual quartz grains as detected from scanning electron microscope (SEM) analysis. These sediment characteristics are used to assess sediment transportation and deposition to trace possible sediment origin. The overall research questions are: (1) When did the sand deposition take place?, (2) Where did the sand originate?, and (3) What do the new data tell us about the palaeoenvironment at Raunis?

Location and general geological situation

Raunis (57.17'35.4" N, 25.25'59.6" E, 130 m a.s.l.) is situated 9 km east-south-east of the town of Cēsis, within the northern part of the Vidzeme Upland in central–north-eastern Latvia (Figure 1a). The section is located on the eastern bank of the River Raunis, which occupies a former ice-moulded depression at the north-west foot of the Upland (Zelčs and Markots 2004) and documents the Raunis paleolake (Figure 1b). The site is located between the Augstroze Interlobate Area and the Sakala Interlobate Upland (Figure 1b), and this upland-lowland alternation, along with the

present-day topography of Latvia, is due to the oscillatory retreat of the Late Weichselian Scandinavian Ice Sheet and its ice lobes (Zelčs and Nartišs 2014). The northern foothill of the Vidzeme Upland, which was located in the Rīga-Peipsijärv interlobate area during the Late Weichselian, was exclusively shaped by the Burtnieks ice lobe with its numerous ice tongues: the Amata, Abuls and Rauna (Zelčs and Markots 2004), and this latter lobe is likely responsible for glacial deposition in the Raunis area.

The Vesselava end-moraine inner margin, belonging to a chain of the Linkuva ice-marginal zone and the Rauna ice tongue, is located only a few kilometres to the south-east from Raunis, followed by the Dzirnupe–Upper Vaive meltwater drainage valley and the Mežole Hilly Area (Figure 1b). Dates from the Linkuva zone reveals a wide distribution between 15.4 ^{10}Be and 12.0 ^{10}Be ka (Zelčs et al., 2011) that corresponds to c. 17.5 and 13.7 recalculated ^{10}Be ka ages (Hughes et al, 2016). So far no attempts to narrow this age span have been made. Recent compilation reconstructions of the deglaciation of the Fennoscandian ice sheet place the deglaciation of the Raunis area at c. 15 ka (Stroeven et al. 2016) and c. 16 ka (Hughes et al. 2016), respectively.

In general, three lithological units can be visually distinguished at Raunis, and these are two diamict units (1 and 3) with organic sediments (unit 2) in between (Figures 2a, 3 and Table 1). Details on them are given in the following sections.

Previous studies

Several radiocarbon ages from the organic sediments (unit 2, Figures 2A-B and 3) at Raunis are available from previous studies (see Figure 1b for sites location). The silty organic-rich horizon, re-dated in this study (AMS sample in unit 2, Figures 2a and 3), has so far received the most attention in terms of dating (Table 2). The very first radiocarbon dating attempts of the Raunis section in the 1960s gave an age of 16,086±1552 cal y BP (13,390±500 y; Mo-296; Vinogradov et al. 1963), which agrees with dating results of remains of *Sphagnum* and green mosses (Ta-177; 15,862±493 cal y BP; 13,250±160 y) obtained by Punning et al. (1968). A later conventional radiocarbon date

resulted in a similar age of 16,024±753 cal y BP (13,320±250 y; Ri-39; Stelle et al. 1975a, 1975b). Significantly younger ages of 12,598±509 cal y BP (10,780±220 y; Ri-5) and 12,116±927 cal y BP (10,400±370 y; Ri-5A) were obtained by Zobens et al. (1969). Dating of deformed and partially disrupted peat at a depth of 0.75-1.5 m gave a result of 8,837±198 cal y BP (8,020±70 y; Zelčs and Markots 2004). Later ages reported by Raukas (2009) cover the Early Holocene time span with results of 10,478±217 cal y BP (9302±83;Tln-2319) and 10,401±156 cal y BP (9227±70 years; Tln-2322), which coincides with the pre-Boreal time frame as reported by Jakubovska and Stelle (1996) and Stelle et al. (1999). Finally, the latest datings as provided by Amon (2011; unpublished data) gave two ages of 13,197±127 cal y BP and 13,266±140 cal y BP (11,350±70 y, Poz-38330 and 11,420±60 y; Poz-38331, respectively).

Along with radiocarbon dating, numerous palaeobotanical study were carried out, stating that a rapid succession from an open subarctic to boreal vegetation took place during the deposition of the organic beds (Ceriņa et al. 1998b, 1998a; Ceriņa and Kalniņa 2000), and flora constituents argue for a Late Glacial origin (Kalniņa et al. 2011). Finally, clastic sediment studies of the overlying diamicton revealed a limited horizontal extent (Ceriņa et al. 1998a, b). Together with fabric orientations unrelated to glacial movement, this suggests that the diamicton is not of glacial origin, but is the result of slumping and/or redeposition (cf. Danilans 1973).

Material and methods

Sedimentology

All visible clastic horizons or lenses thicker than 7-8 cm were subjected to sampling at the Raunis site, resulting in nine sediment samples of 300–400 g each (labeled as R1-R9, Figs. 2A, 3; Table 1), except of sample R3, where only ca. 50 g of material was collected due to the relatively thin sand horizon. In the laboratory, this material was subsampled and ca. 150–200 g material (50 g for R3 sample) was mechanically dry sieved to obtain the 0.5–1.0 mm fraction for further SEM analysis.

A total of 180 quartz grains (20 grains/sample) were analysed by SEM (Zeiss EVO MA 15) at the Department of Geology, University of Tartu, Estonia. Grains were randomly selected and placed on SEM stubs without prior coating, and further pictured at ca. 100x magnification for a general grain outline and ca. 400–1500x to distinguish microtextures, following recommendations of Mahaney (2002). Later, the semi-quantitive approach partially following Vos et al. (2014) was used, where microtextures were grouped depending on their frequency as follows: >75% – abundant (occurrence); 50–74% – common; 26–49% – moderate; 6–25% – sparse; <5% rare, and 0% – not observed.

Optically stimulated luminescence and radiocarbon dating

Eight samples were OSL dated from units 1-3 and labelled as Lund-16001-08 (Figures 2A, 3 and Table 2). These samples correspond to some extent with above mentioned R1-9 samples, except of sample R3 (unit 3a). Here, no OSL sample was obtained (but 50 g for SEM analysis, *see* Sedimentology), since the sand lens was too thin. Sediments for OSL dating were obtained from the pit by hammering plastic tubes into a clastic sediment horizon. After recovering the tube, both ends were instantly capped to prevent light exposure.

Sample preparation and OSL measurements took place under subdued red light at the Lund Luminescence Laboratory, Sweden. At first, the samples were wet sieved to recover the fraction of either 180–250 µm or 63–90 µm, depending on the sediment grain-size distribution. This latter fraction is particularly relevant to the Lund-16001 sample, where the amount of medium and fine sand was low, contrary to abundant very fine sand fraction. Sediment in the ends of the tubes (ca. 30 mm) was removed due to the possibility of uncontrolled bleaching during sampling, and further used for measurements of dosimetry and moisture content.

Sieved fractions were dried and chemically treated with 10% hydrochloric acid (HCl), 10% hydrogen peroxide (H_2O_2) and heavy liquid (LST Fastfloat, ρ=2.62 gcm^{-3}) to remove carbonates and organics and to separate quartz from lighter minerals including K-feldspar. After this, quartz

extracts were treated with 38% hydrofluoric acid (HF) and again by 10% HCl. All samples, except Lund-16001, were dry re-sieved to remove any <180 µm grains. All equivalent dose measurements were performed on large (8 mm) aliquots of quartz utilizing a Risø TL/OSL DA-20 reader with a $^{90}Sr/^{90}Y$ beta radiation source. Initial IR-tests showed that most samples were affected by significant feldspar contamination (infrared/blue signal ratio >10%), particularly Lund-16004 and 16008. Post-IR blue stimulation (Banerjee et al. 2001) was therefore used for dose determination, except for samples 16004 and -08, which were measured with pulsed stimulation (Ankjærgaard et al. 2010). Dose recovery ratios at different preheat temperatures along with standard preheating plateau test were measured for three aliquots per temperature for the Lund-16003 sample. Altogether 15 aliquots covered the temperature range between 180 ºC and 260 ºC with an interval of 20 ºC. As a result, a preheating temperature of 200 ºC, with a 180 ºC cutheat was chosen. The single aliquot regeneration protocol settings (Murray and Wintle 2000, 2003) were tested with dose recovery tests for all samples and the mean measured/given dose ratio (0.96±0.0975; n=24) show that the protocol can retrieve a given dose. The luminescence signal was obtained from channels 1 to 5 (=the first 0.8 s) for the peak, and channels 6 to 10 (=the next 0.8 s) for background. Aliquots were accepted if the recycling ratio was within 10% of unity and test dose error ≤10%. For samples 16001, -04, -05 and -07 the dose showed a significant dependence on apparent feldspar contamination and an additional rejection criterion based on the ir/blue ratio was used. Dose calculation was done by exponential curve fitting in Risø Analyst v. 4.31. The central age model (CAM) was applied, and, the minimum age model (MAM) with three parameters (Galbraith et al. 1999) was also used where recommended according to the Arnold et al. (2007) decision protocol for single aliquots. Only MAM-3 doses with p-values close to 1 were accepted.

Subsamples from one tube end were subjected to dose rate measurements. This part of the material was first dried at 105ºC for 24h, then ashed at 450ºC for 24h, mechanically ground and finally, cast in wax in a defined geometry. Casts were further stored for at least 3 weeks and radionuclide concentrations were measured using high-resolution gamma spectrometry at the Nordic Laboratory

for Luminescence Dating, Denmark (Murray et al. 1987). The environmental dose rate was then calculated using the DRAC online calculator (Durcan et al. 2015).

Sediment from the other end of the tubes was weighed and considered to represent the natural water content. After 24h of saturation in water the saturated water content was measured as weight of water per dry mass (weighed after 24h of 105 ºC drying). The natural and saturated water content ranges between 2% and 70%, and both these values are unlikely as long-term water content. Therefore, a value somewhere between saturated and natural water content must considered as life-time average burial water content. Our natural water content measurement, as measured on separate samples taken in the winter season, varied between 10% (sample Lund-16002) and 45% (Lund-16001), and these values were considered as representative of a long-term water content and accordingly implemented into the age calculation.

In addition to the OSL dating, one bulk silty organic sample (AMS in unit 2, Figs. 2A, 3) was collected for AMS radiocarbon dating, as performed at the Radiocarbon Dating Laboratory, Lund University, Sweden, and further calibrated using IntCal 4.3 (Ramsey 2017).

All existing radiocarbon ages of Raunis were recalibrated using Oxcal 4.3 (Ramsey 2017) to make them comparable to each other and suitable for comparison with OSL ages. The calibrated ages are used in the text and provided in Table 2 along with their uncalibrated versions.

Results

General sediment characteristics

At Raunis section, two brownish diamict beds constitute the bottommost (unit 1) and uppermost (unit 3) part of the profile. The two beds are folded. Distinction between unit 3a and b was apparent from sediment deformations that occur in unit 3b, but are absent in unit 3a. Between unit 1 and 3 a complex alternation of numerous yellowish and brownish sandy horizons and lenses with sandy peat-gyttja-clay layers occurs (unit 2; Figures 2a–g and 3). The clastic components in unit 2

constitute in general massive or vaguely laminated sand horizons and lenses (Figure 2 c–e). However, a closer inspection reveals reverse grading, randomly distributed pebbles (Fig. 2B; F–G), and clayey intraclasts (Figure 2b-e). Contacts between organic components and sand components are either sharp or gradual (Figure 2 c–d). Additionally, small faults (up to few tens of centimetres displacement) along with sediment deformations occur occasionally in unit 2 (Figure 2B; e–g).

Grain characteristics in SEM

Subangular grains are the main constituents of sand deposits in all three units (Figure. 4 and 5a, b), followed by rounded grains (Figure 4 and 5c). Angular grains (Figure 5d) occur sparsely, rarely or are absent except for R5 (Lund-16006), where angular grain occurrence is moderate, and strongly accompanied with, for example, flat cleavage surfaces (Figure 5e) and big (>100 µm) conchoidal features (Fig. 5f). Among the microtextures of mechanical origin crescentic marks dominate (Figure 5g, h), generally followed by differently-sized conchoidal features (as mentioned), V-shaped percussion marks (Figure 5i) and arcuate (Figure 5j) and straight steps (Figure 5k). Nevertheless, the general pattern is that rounded grains are associated with V-shaped marks and dull surfaces (i.e. samples R1, R4, R6-8). This dullness occurs on many grain surfaces (Figure 5l, m). Many grains also carry microtextures of chemical origin such as solution pits and crevasses, which occur on grain surfaces mostly accompanied by silica precipitation (Figure 5l-m). Occasionally, these pits are oriented (Figure 5n). Particularly, R8 and R9 reveal numerous grains with low relief (Figure 5o). This is in contrast with R1, 4 and 5, where practically no low-relief grains have been observed in the sediments, but rather moderate relief, along with some high relief grains (Figure 5p).

Luminescence and radiocarbon dating

The OSL samples have a sensitivity of 45-190 counts Gy^{-1}, meaning that samples are dim or fairly dim, which prevented measurement of small aliquots. The mean equivalent doses present a wide range between 33±2 Gy and 208±16 Gy (Table 3), and some of the aliquots with high doses are

close to or at saturation. The environmental dose rates vary between 1.49±0.10 Gy ka^{-1} and 2.70±0.08 Gy ka^{-1} . The resulting ages range from 12.0±0.6 ka to 122±9 ka, with the majority between 59 ka and 27 ka (Table 3). In some cases, the value of the overdispersion (OD) is high, between 40±6% and 60±8.5% (samples 16002, -03, respectively; Table 3). The dose distribution of four samples is skewed with skewness values between 0.62 (sample 16002) and 4.69 (16003); for these the MAM3 was applied, but it provided reliable results for only two of the samples (16002, 03). The MAM3 ages are preferred for these samples, but overlap the CAM ages within error (Table 3). The AMS radiocarbon dating gives a result of 14,025±270 cal y BP (LuS 13695; Table 2).

Discussion

Depositional environments

Sedimentary structures along with the shape and surface texture of quartz grains provide excellent information about their history and depositional environments (Alhazza et al. 2019; Costa et al. 2017; Kalińska-Nartiša et al. 2016a, 2018; Mahaney et al. 2004; Woronko 2012; Miall 1985). In this section, samples are discussed according to their possible origin. Since aquatic quartz grain origin prevails in most of the investigated samples, these samples are discussed first. Glacial grain origin is minor and appears only in grains of the sediment sample R5 (Lund-16004; Figs. 2, 5e). Five samples carry a low feature intensity of their quartz grains, and are therefore likely related with a low-energetic aquatic depositional environment. These are samples R1 (=Lund-16001), R2 (=Lund-16002), R3, R4 (=Lund-16003) and R9 (=Lund-16008). Similarly, massive or vaguely laminated sand horizons as observed generally within unit 2 (samples R1 and R2) are from low-energy water conditions. Studies of the organic sediments at Raunis (Ceriņa et al. 1998b, 1998a; Ceriņa and Kalniņa 2000) point at lake deposition, and the scarcity of microtextures on grains from samples R1 and R2 support this. On the other hand, inverse grading occurs sometimes in these sand layers, which means that the coarser grains preferentially roll over finer grains (cf. Phantuwongraj

et al., 2013) and environmental energy increased with a time (Weckwerth, 2018).

Sandy material from samples R8 and R9 (Lund-16007 and -08, respectively; Figs. 2A, 3) carries the lowest number of quartz grains with high surface relief among all investigated samples, and grains have practically no fresh conchoidal features. Because the grain surface is dulled, sediment deposition took place under aquatic conditions (Widdowson 1997; Kalińska-Nartiša et al. 2017a) of low energy and/or long distance. Nevertheless, fluvial collision contributed to their shaping, because numerous crescentic marks occur (Vos et al. 2014). Importantly, in case of sample R9, a glacigenic grain record with high pressure fracturing such as straight and curved grooves and chattermarks (Kar et al. 2018; Mazumder et al. 2017) should be expected due to the proximity to unit 1, which has been interpreted as a basal till bed by Zelcš and Markots (2004). Instead, these grains originate from an aquatic environment of relatively low energy. This may point at reduced shear stress in the glacier (Mahaney 2002), due to limited thickness (Mahaney et al. 1996), or ice-marginal conditions with limited time to produce high stress microtextures (Kalińska-Nartiša et al. 2017a, b), or not directly glacial, but, for example, (glacio)lacustrine depositional environment, which is at odds with the interpreted till origin of unit 1 (Zelcš and Markots 2004). Since this till bed has so far not been studied in detail, we lack sufficient information for further interpretation.

Our grain data from unit 3 do not provide conclusive evidence in either direction. A pseudoglacial origin, related to slope processes and redeposition as already suggested earlier (Danilans 1973; Zelcš and Markots 2004) may be supported by sample R7 from sand interlayers in unit 3b. Sample R7 carries non-glacial, aquatic grains with the highest number of V-shaped percussion cracks, meaning that aqueous environment must have been high energetic (Gobala krishnan et al. 2015; Mahaney 2015; Margolis and Kennett 1971), and likely related to turbulent meltwater. On the other hand, sample R5 (Lund-16004), also from unit 3, is the only sample that carries a glacial quartz grain record, where subangular and angular grains with fresh conchoidal features, steps and some deep grooves dominate, as typical for glacial environments (cf. Hart 2006).

Sample R7 carries aquatic grains with the highest the highest number of V-shaped percussion

cracks, meaning that aqueous environment must have been high energetic (Gobala krishnan et al. 2015; Mahaney 2015; Margolis and Krinsley 1971), and likely related to turbulent meltwater. Among all investigated clastic horizons, only sample R5 (Lund-16004) from unit 3a carries glacial quartz grain record, where subangular and angular grains with fresh conchoidal features, steps and some deep grooves dominate, as typical for glacial environments (cf. Hart,2006).

Chronological record of sandy and organic horizons

A total of eight OSL samples were dated from sandy horizons and lenses at Raunis section, and these dates are generally older than expected from previous studies. Most of the obtained ages fall in the Middle Weichselian/MIS 3 (59-27 ka) and one is apparently of last interglacial age (122±9 ka; 16002). If taken at face value, the ages are not in stratigraphic order (Figure 2) and a careful evaluation of the data is therefore required.

In general, we consider our OSL data as technically correct, since a fast OSL signal component dominates (Figure 7) in all investigated samples and standard methodological criteria (Murray and Wintle 2000, 2003) are fulfilled. However, there are some issues that complicate matters, and lead us to the consider only one out of the eight ages to be reliable. These issues are 1) incomplete bleaching, 2) saturation and 3) dose rate, and these are further discussed below.

Based on the interpretation of the depositional environment of the sampled sediments as discussed above (cf. Danilans 1973) there is a risk that these sandy sediments might not have been properly bleached while deposited. Problem of poor sediment bleaching in some depositional environments have been already raised, for example by Weckwerth et al. (2012), and in the Baltics region, this seems to be a serious case in glacial-related sediments (Kalińska-Nartiša et al. 2016b, 2015; Raukas et al. 2010; Lamsters et al. 2017).

The effect of incomplete bleaching can be assessed in different ways, for example by analysing dose distributions of individual samples (Bailey and Arnold 2006) or stratigraphic consistency of multiple samples (Banerjee et al. 2001). In this study, the stratigraphic order is broken by the ages

from unit 2, which include both the youngest (12.0±0.6 ka, 16001) and the oldest (121.6±8.6 ka, 16002) age. With its non-skewed dose distribution and low overdispersion we argue that sample Lund-16001 (12.0±0.6 ka) is the most reliable among the eight OSL-dated samples. If we assume that sample 16001 from unit 2 is correct, the ages from the overlying unit 3 as well as the other age from unit 2 must all be too old. The dose distribution data, though limited by the averaging among grains that occur for large aliquots (Duller 2008), support this interpretation. Four of the samples (Lund-16002, 03, 05 and 06) do have significantly positively skewed dose distributions, which we interpret as caused by incomplete bleaching. Additionally, the overdispersion (OD) is larger than for well-bleached samples (Arnold and Roberts 2009) for all samples (Figure 6), except Lund-16001 (16±3.4%), though high OD values may have other causes than incomplete bleaching only (Zhang et al. 2003). Samples 16004 and -08, in particular, have very wide dose distributions, covering a range of >200 Gy (Figure 6), leading to large uncertainties for the equivalent doses. The Minimum Age Model (MAM-3, Galbraith et al. 1999) was applied to the four samples with skewed dose distributions to identify the youngest, thus likely better bleached dose population to provide a more accurate age. However, the MAM-3 provides reliable results only for two samples (16002, -03), both of which overlap with the corresponding CAM age within 1-2 σ. For the other samples probability (p) values are very low, meaning that ages obtained from the MAM-3 are not reliable and that we cannot account for the effect on incomplete bleaching in a good way. Interestingly, and partly contradictory, the grouping and overlap within errors of ages within units or sub-units (16003+04 (3a) and 16006+07 (3b); Figures 2, 7 and Table 2) could be used as support for the accuracy of these ages. However, there is still an age inversion from unit 2 to unit 3. A possible explanation for this is that the timing of the last exposure to light, which the OSL ages record, is not the timing for the last deposition for the unit 3 sediments, which are interpreted as deposited in glacial environments and/or being reworked (see above). These OSL ages would in that case reflect an earlier event, and only provide maximum ages for the deposition of unit 3. Saturation is another issue to consider for reliable dose determination, and if present would imply

that the ages are minimum ages only. Quartz typically saturates at around 150 Gy (Chapot et al. 2012; Timar-Gabor et al. 2010) and four of our samples have mean doses higher than this (16002, -03, -04 and -08; Table 3). However, looking at individual aliquots, there are not many of them that have equivalent doses larger than $2D_0$ and thus should be considered at or close to saturation (Wintle and Murray 2006). For sample 16002 it is five of the accepted aliquots, for samples 16003 and 16004 only one out of a total of 31, 27 and 36, respectively. Saturation, and the risk of the ages being minimum ages, is therefore not regarded as a problem for these samples.

The environmental dose rate is an important part of the luminescence age calculation and errors in its estimation can result in erroneous ages, either too young or too old. For the Raunis samples, there are two aspects of the dose rate estimation that lead to the main uncertainties: water content estimates and sediment heterogeneity.

The value for sediment water content that goes into the age equation is the average water content since time of deposition, which is difficult to estimate. A discrepancy of 1% from the true water content over time results in a 1% deviation from the true burial age (Kenzler et al. 2016), with higher water content making the age older and vice versa. We have used the field water content and the saturated (maximum) water content as limits for the probable average water content and estimated a likely value in between these, based on the sediment and its setting (Table 3). If we instead choose to use the field water content or the saturated water content as average water content, the ages remain within 2σ of the chosen value for all samples but two (16001 and -04) and are thus not statistically significantly different. For sample 16001 the discrepancy is at least partly due to the high saturated value (70%), which is caused by the presence of organic matter in the bed. From the topographic setting and geological history of the sediments, we consider water contents close to saturation as unlikely for average water content and, consequently unlikely that the ages are overestimated due to this.

The sediments at the Raunis section are heterogeneous, with interbedded clay, sand and gyttja (Fig. 2). We have sampled the sandy beds for OSL-dating, but these beds are quite thin and the quartz

grains in them will thus be exposed to radiation also from surrounding beds, which may be lithologically different. Our background samples, which were used for gamma spectrometry and determination of the sediment dose rate, mainly consist of sand, with little representation of e.g. the clayey beds. Though most of the irradiation still comes from the near distance to the sample, i.e. within the sand, and there also is similar sand in beds above and below the sampled bed, this adds uncertainty to our ages, particularly to those from the thinnest sand beds (16002, -03). However, we estimate the effect to be limited, though not necessarily insignificant.

Summing up, we consider the effect on incomplete bleaching to be the largest problem for the set of OSL ages from Raunis. Mainly on the basis of the character of their dose distributions (skewed and/or wide), we must disregard the ages from most of the samples (16002-06 and 16008). Samples 16001 and 16007 are from a methodological perspective considered the most reliable ages, but they are not in stratigraphic order (Table 3) and so both cannot be true depositional ages.

Of the two, we favour sample 16001. For this sample from unit 2, dated to 12.0±0.6 ka, there is independent chronological data to compare with and which supports its young age. Unpublished AMS datings, from the same unit, of ca. 13,300–13,200 cal y BP, provided by Amon (2011), indicate that the organic horizons accumulated in the warmest part of the Allerød at 13,000–12,700 cal y BP (Veski et al. 2012). Our new, single radiocarbon age suggests that organic deposition took place 700–800 years earlier at 14,025±270 cal. y BP, which falls into end of the Bølling warming (Lowe et al. 2008; probably analogous to Greenland Interstadial 1e – GI-1e, cf. Cook et al. 2018). None of these dates correspond within 1 σ, but within 2 σ, to the OSL age, coming from a sand bed just below the organic beds in unit 2 (Figure 3). It is widely accepted that age inversion within 1-2 σ, as in this study, most likely does not show a statistical difference, thus may be considered as identical (cf. Halfen et al. 2012). Nevertheless, we can discuss possible reasons for the difference. Causes for the luminescence results being slightly too young could be dose rate uncertainties as discussed above. Too old AMS radiocarbon ages could be related to reservoir and hard water effects, as also observed in a regional studies by Koff and Terasmaa (2011), Poska and Saarse

(2002) and Stivrins et al., (2016), and which our bulk sediment sample would be easily subjected to.

Raunis stratigraphy and context

Numerous stratigraphic schemes and concepts have been applied to the climatic fluctuations of the Late Glacial (analogous to Greenland Interstadial GI-1 and up to Greenland Stadial GS-1; (Cook et al. 2018; Heiri et al. 2014; Rasmussen et al. 2014). Some of these concepts raise much confusion (see for details de Klerk 2004), and the Raunis Interstadial clearly belongs to this group. First mentioned by Savvaitov and Straume (1963) and Savvaitov et al. (1964), this interstadial was used as evidence for an early warm period prior to the Bølling (likely analogous to Greenland Interstadial GI-1e), which according to Dreimanis (1966) is correlated with the Susacá Interstadial as also observed by Van der Hammen and Vogel (1966) in South America. The Raunis section is controversial and numerous scenarios have so far been suggested (see Earlier age determination and sediment study). The Raunis section carries a number of deformed and overturned organic and clastic beds, which raised the question whether this organic horizon may be possibly a raft of interstadial/glacial sediments glacially thrust from the buried Raunis valley (Dreimanis and Zelčs 1995).

Following all these assumptions along with radiocarbon dating results from previous studies and this study, we expected a Late Glacial time frame of the OSL ages from sediments from the same unit (unit 2, sample 16001) and above (unit 3, samples 16002-07) the organic complex, and likely an age older than the Late Glacial of the underlying sediments (unit 1, sample 16008). This is partly true: unit 1 is dated to the Middle Weichselian (59.2±6.9 ka) and both the organic horizon and sand horizon of unit 1 have ages falling into Greenland Interstadial 1 (=likely Late Glacial). However, a more detailed correlation is hampered by the resolution of the ages and the problems with incomplete bleaching, as discussed above. Trusting only one of the OSL ages (16001) and the new radiocarbon age, we can therefore only reliably discuss the chronology of Raunis unit 2.

Unit 2 consists of sand-gyttja beds with organic horizons, and it is dated to 12.0 ± 0.6 and 121.6 ± 8.6 ka by OSL and to 14,025±270 cal. y BP by radiocarbon. As discussed above, we consider the

young OSL to provide the most accurate age. This OSL result correlates with the onset of the Younger Dryas cold period (Van Hoesel et al. 2014), which is at the transition between Greenland Interstadial 1a and Greenland Stadial 1 (GI1; Rasmussen et al. 2014). The sedimentary record clearly argues for lake deposition as seen through the occurrence of gyttja and quartz grain microtextures such as dulled grains surfaces. Such surfaces, with a limited number of mechanical features, indicate a low-energy aquatic environment. In this time frame aeolian activity took place in the territory of Latvia, and particularly at 12.8–12.3 ka aeolian sedimentary structures and landforms developed (Kalińska-Nartiša et al. 2016b). Nevertheless, no quartz grains with aeolian imprint have been found in the lake unit. The other sample from Unit 2 (R2/16002) likewise has grain characteristics of a very low energetic environment, but its age is vastly overestimated compared to sample 16001. At the current state of this study, we do not observe any relation between bleaching characteristic and quartz grain surface character. Closer inspection may reveal higher grain relief and microtexture frequency in case of the well-bleached sample R1 (16001) comparing with the rest investigated samples. However, this requires future attention. Generally this sample, which appears fine, does not sedimentologically differ from the others. This clearly shows that there are no clear rules while using luminescence methods in some sedimentary settings and localities.

Since no reliable ages were retrieved from units 1 and 3 we only briefly speculate about their absolute chronology and sedimentary context. Unit 1 is underlying the 12-14 ka old Unit 2 and is at face value dated to 59.2±6.9 ka (16008, Table 2). This is in stratigraphic order and its apparent age would fall close to the boundary of marine isotope stages 3 and 4 (MIS 4/3), and the Middle Weichselian glaciation (60-50 ka) in northern Eurasia (Svendsen et al. 2004). At Raunis, the sedimentological information from the quartz grains suggests a low-energy aquatic environment, but previous studies (Zelčs and Markots, 2004) considered unit 1 to consist at least partly of till, making the age reasonable in the context, though still methodologically unreliable. We can therefore only conclude that Unit 1 is older than 12-14 ka.

Quartz grains from the sand lens in unit 2 dated to 121.6 ± 8.6 ka (sample 16002) have similar characteristics of a very low energetic environment, which is clearly supported by a lack of V-shaped percussion marks. However, the 122 ka is likely a vast overestimate (see above), and sediment deposition likely took place at around 12 ka. On the other hand, accepting a date of 122 ka would support the idea of Dreimanis and Zelčs (1995) about a possible raft of glacial sediments and thrusted from the buried Raunis valley.

Unit 3, overlying Unit 2, should be younger than 12-14 ka, but ages are significantly older: 34-49 ka for unit 3a and 27-30 ka for unit 3b. The sedimentary evidence suggest that these sediments may have been reworked, for example by slumping as suggested by Danilans (1973), where no light exposure took place and the dated sediment would therefore be expected to be poorly bleached or even unbleached during its most recent deposition. The broad and skewed dosed distributions and the age overestimation compared to the underlying unit supports this. Considering the topographically lower location of the Raunis along with a proximity of the Vesselava end moraine, slumping material may had originated from this, and the one age from Unit 3 that is considered technically reliable (16007; 27 ka) is interpreted as a maximum age of the deposition of the unit.

Conclusions

In this study, the clastic beds at Raunis, central Latvia are subjected to age determination and palaeoenvironmental interpretation for the first time, and we distinguish three units, which we discuss and place in a regional context. Fast component OSL signal prevails in all investigated samples, but equivalent dose distributions reveal large overdispersion and significant skewness for several samples. Therefore, it is likely that most OSL ages suffer from incomplete bleaching and apparent age overestimation and only provide a maximum age of sediment deposition. The most reliable OSL age, 12.0±0.6 ka, from unit 2 just corresponds within 2 sigma with a new AMS result (14,025±270 cal y BP), from an adjacent organic horizon from the same unit. The OSL date may be slightly too young or the AMS date slightly too old. We consider the OSL age to be most accurate, and that the radiocarbon age appears slightly too old due to reservoir and hard water effects, which

are known from the region.

The lowest unit, Unit 1, has an OSL age of c. 59 ka and reveals sediment deformation and likely subglacial deposition with a limited shear stress, because sand quartz grains suggests a record of a low-energy aquatic environment on their surfaces. The age is considered unreliable and the unit .

Unit 2 consists of sand-gyttja alternation, and clearly points at lake deposition. Observed quartz grains have dulled surfaces with a limited number of mechanical features. This unit is dated to 14-12 ka, meaning that organic-sandy sediments were generally accumulated during the Greenland Interstadial 1 (GI-1). Another sand lens reveals an unreliable OSL age of 122 ka.

The top unit, unit 3, has been reworked and its sediments most likely experienced a limited sun exposure and thus the obtained OSL ages, of which only one (27 ka) is considered reliable, would be maximum sediment ages only.

Considering the above mentioned bleaching problem, luminescence age overestimation and sediment properties combined with previous studies at Raunis, we consider this site largely questionable as a stratigraphic key site. This has implications for further regional correlation.

Acknowledgements

Māris Nartišs (University of Latvia) is thanked for discussion and help in the field. Jacob Hardt and an anonymous reviewer are thanked for valuable comments that improved the final version of the manuscript. This research was supported by the Research University – Initiative of Excellence: the Emerging Field “Global Environmental Changes” and "CatFlood Research Team" at Nicolaus Copernicus University in Toruń.

Figure and table captions:

Figure 1. (a) Map of the study area with respect to major glacial landforms. AI – Augstroze

Interlobate Area; SU – Sakala Interlobate Upland. B – Map of the Raunis palaeolake area. 1 - Mežole Hilly Area; b - Dzirnupe – Upper Vaive meltwater drainage valley; 3 – Veselava end moraine; 4 - palaeolakes – R - Raunis; M - Mīlīši; black square - ^{14}C sampling sites from 1963 to 1975 and in this study; white square - C14 and sampling site in 2008 and 2010; black dots - outcrops with interlayers of plant remains. Digital elevation model is derived from topographic maps of scale 1:10,000.

Figure 2. (a) Overview photo of the Raunis section with sampling points (small white circles – samples R1-R9 for SEM analysis; big white circles – samples Lund-16001-09 for OSL dating; big white rectangle – AMS sample) and the 1-3 units; (b)–(g) a closer look at parts of the section: (b) peat-gyttja-clay-sand interbeds with random pebbles in sand part and faults (unit 2); (c)–(d) sharp and gradual contacts between gyttja and sand components (unit 3a); (e) sediment deformations in unit 3a; (f)–(g) sediment deformations in unit 1.

Figure 3. General unit log of the Raunis section showing its age and environmental interpretation Sediment log of the investigated Raunis section. Results of the OSL (black circles) and AMS (black square) datings from different levels of the section are indicated.

Figure 4. Frequency of selected grain microtextures from SEM along with their origin.

Figure 5. SEM quartz grain micrographs of the investigated samples: (a)–(b) subrounded grains; (c) rounded grain; (d) angular grain; (e) flat cleavage surface (arrow); (f) big (>100 μm) conchoidal features (arrow); (g) crescentic marks on a whole grain surface; (h) details on crescentic marks; (I) V-shaped percussion marks (arrows); (j) straight steps (arrows) visible on a conchoidal feature; (k) arcuate steps (arrow) on a conchoidal feature; (l)–(m) solution pits and crevasses, accompanied by silica precipitation (in depressions) and dulled surfaces (on corners; arrows); (n) oriented etch pits; (o) grain with low relief; (p) grain with high relief.

Figure 6. The D_e distributions of all samples shown as histograms and radial plots. Please note different scale for axes.

Figure 7. Example of growth (a) and decay (b) curve from OSL sample Lund-16001.

References:

Alexanderson H, Backman J, Cronin TM, Funder S, Ingólfsson O, Jakobsson M, Landvik JY, Löwemark L, Mangerud J, März C, Möller P, O'Regan M, Spielhagen RF. 2014. An Arctic perspective on dating Mid-Late Pleistocene environmental history. Quat Sci Rev. 92:9–31. DOI:10.1016/j.quascirev.2013.09.023.

Alhazza A, Ahmad S, Al-Dousari A. 2019. Characterization of sand particles in arid areas. In: Boughdiri M, Bádenas B, Selden P, Jaillard E, Bengtson P, Granier BRC. (Eds.), Paleobiodiversity and Tectono-Sedimentary Records in the Mediterranean Tethys and Related Eastern Areas. Springer International Publishing, Cham:335–337.

Amon L. 2011. Palaeoecological reconstruction of late-glacial vegetation dynamics in eastern Baltic area: a view based on plant macrofossil analysis, PhD thesis. Tallinn University of Technology, Tallinn.

Anisimov M, Tumskoy VE. 2002. Environmental history of the Novosibirskiye Islands for the last 12 ka. Terra Nostra. 3: 22–23.

Ankjærgaard C, Jain M, Thomsen KJ, Murray AS. 2010. Optimising the separation of quartz and feldspar optically stimulated luminescence using pulsed excitation. Radiat Meas. 45:778–785. DOI:10.1016/j.radmeas.2010.03.004.

Arnold LJ, Bailey RM, Tucker GE. 2007. Statistical treatment of fluvial dose distributions from southern Colorado arroyo deposits. Quat Geochronol. 2:162–167. DOI:10.1016/j.quageo.2006.05.003.

Arnold LJ, Roberts RG. 2009. Stochastic modelling of multi-grain equivalent dose (D_e) distributions: Implications for OSL dating of sediment mixing. Quat Geochronol. 4(3):204–

230. DOI:10.1016/j.quageo.2008.12.001.

Bailey RM, Arnold LJ. 2006. Statistical modelling of single grain quartz D_e distrbutions and an assessment of procedure for estimting burial dose. Quat Sci Rev. 25:2475–2502. DOI:10.1016/j/quascirev.2005.09.012.

Banerjee D, Murray AS, Bøtter-Jensen L, Lang A. 2001. Equivalent dose estimation using a single aliquot of polymineral fine grains. Radiat Meas. 33:73–94. DOI:10.1016/S1350-4487(00)00101-3.

Battarbee RW. 2000. Palaeolimnological approaches to climate change, with special regard to the biological record. Quat Sci Rev. 19:107–124. DOI:10.1016/S0277-3791(99)00057-8.

Bitinas A. 2012. New insights into the last deglaciation of the south-eastern flank of the Scandinavian Ice Sheet. Quat Sci Rev. 44:69–80. DOI:10.1016/j.quascirev.2011.01.019.

Ceriņa A, Danilans IJ, Dreimanis A, Jakubovska I, Stelle V, Zelčs V. 1998a. Raunis late glacial deposits southeastern from Cesis. In: Field Symposium on Glacial Processes and Quaternary Environment in Latvia, 25-31 May 1998. Excursion Guide:66–73.

Ceriņa A, Jakubovska I, Savvaitov AS, Stelle V. 1998b. Raunis interstadial deposits in Latvia. In: Field Symposium on Glacial Processes and Quaternary Environment in Latvia, 25-31 May. Abstracts of Papers and Posters. University of Latvia, Riga:8–10.

Ceriņa A, Kalniņa L. 2000. A new investigation of sections on the right bank of the Raunis River. In: Latvijas Universitates 58. Zinatniskas Konferences Zemes Un Vides Zinatnu Sekcijas Referatu Tezes. University of Latvia, Riga:29–32.

Chapot MS, Roberts HM, Duller GAT, Lai ZP. 2012. A comparison of natural- and laboratory-generated dose response curves for quartz optically stimulated luminescence signals from Chinese Loess. Rad. Meas. 47:1045–1052. DOI:10.1016/j.radmeas.2012.09.001

Cook E, Davies SM, Guðmundsdóttir ER, Abbott PM, Pearce NJG. 2018. First identification and

characterization of Borrobol-type tephra in the Greenland ice cores: new deposits and improved age estimates. J Quat Sci. 33:212–224. DOI:10.1002/jqs.3016

Costa PJM, Gelfenbaum G, Dawson S, Selle S La, Milne F, Cascalho J, Lira CP, Andrade C, Freitas MC, Jaffe B. 2017. The application of microtextural and heavy mineral analysis to discriminate between storm and tsunami deposits. Geol Soc London, Spec Publ. 456. DOI:10.1144/SP456.7

Danilans IJ. 1973. Quaternary Deposits of Latvia. Zinātne, Riga.

de Klerk P. 2004. Confusing concepts in Lateglacial stratigraphy and geochronology: origin, consequences, conclusions (with special emphasis on the type locality Bøllingsø). Rev Palaeobot Palynol. 129:265–298. DOI:10.1016/j.revpalbo.2004.02.006.

Dreimanis A. 1966. The Susaca-Interstadial and the subdivision ofthe Late Glacial discussion. Geol en Mijnbouw/Netherlands J Geosci. 45:43–131.

Dreimanis A, Zelčs V. 1995. Pleistocene stratigraphy of Latvia. In: Ehlers, J., Kozarski, S., Gibbard, P. (Eds.), Glacial Deposits in North-East Europe. Balkema, Rotterdam:105–113.

Duller GAT. 2008. Single-grain optical dating of Quaternary sediments: Why aliquot size matters in luminescence dating. Boreas 37:589–612. DOI:10.1111/j.1502-3885.2008.00051.x.

Durcan JA, King GE, Duller GAT. 2015. DRAC: Dose Rate and Age Calculator for trapped charge dating. Quat Geochronol. 28:54–61. DOI:10.1016/j.quageo.2015.03.012.

Galbraith RF, Roberts RG, Laslett GM, Yoshida H, Olley JM. 1999. Optical dating of single and multiple grains of quartz from Jinmium rock shelter, Northern Australia: Part I, Experimetal design and statistical models. Archaeometry 41:339–364. DOI:10.1111/j.1475-4754.1999.tb00987.x.

Gobala krishnan N, Nagendra R, Elango L. 2015. Quartz surface microtextural studies of Cauvery River sediments, Tamil Nadu, India. Arab J Geosci. 8:10665–10673. DOI:10.1007/s12517-

015-1995-0.

Halfen AF, Johnson WC, Hanson PR, Woodburn TL, Young AR, Ludvigson GA. 2012. Activation history of the Hutchinson dunes in east-central Kansas, USA during the past 2200 years. Aeolian Res. 5:9–20. DOI:10.1016/j.aeolia.2012.02.001.

Hart J. 2006. An investigation of subglacial processes at the microscale from Briksdalsbreen, Norway. Sedim. 53:125–146.

Heiri O, Brooks SJ, Renssen H, Bedford A, Hazekamp M, Ilyashuk B, Jeffers ES, Lang B, Kirilova E, Kuiper S, Millet L, Samartin S, Toth M, Verbruggen F, Watson JE, Van Asch N, Lammertsma E, Amon L, Birks HH, Birks HJB, Mortensen MF, Hoek WZ, Magyari E, Munõz Sobrino C, Seppä H, Tinner W, Tonkov S, Veski S, Lotter AF. 2014. Validation of climate model-inferred regional temperature change for late-glacial Europe. Nat Commun. 5:1–7. DOI:10.1038/ncomms5914.

Houmark-Nielsen M. 2010. Extent, age and dynamics of Marine Isotope Stage 3 glaciations in the southwestern Baltic Basin. Boreas 39:343–359. DOI:10.1111/j.1502-3885.2009.00136.x.

Hughes ALC, Gyllencreutz R, Lohne ØS, Mangerud J, Svendsen JI. 2016. The last Eurasian ice sheets - a chronological database and time-slice reconstruction, DATED-1. Boreas 45:1–45. DOI:10.1111/bor.12142.

Jakubovska I, Stelle V. 1996. Peculiarities of fluorescence of polen content from the section on the Raunis River bank. In: LU 55. zinatniska konferences Geografijas un Zemes zinatnu sekcijas tezes un programmas: 21. Latvian.

Kalińska-Nartiša E, Stivrins N, Grudzinska I. 2018. Quartz grains reveal sedimentary palaeoenvironment and past storm events: A case study from eastern Baltic. Estuar Coast Shelf Sci. 200:359–370. DOI:10.1016/j.ecss.2017.11.027.

Kalińska-Nartiša E, Lamsters K, Karušs J, Krievans M, Rečs A, Meija R. 2017a. Quartz grain

features in modern glacial and proglacial environments: A microscopic study from the Russell Glacier, southwest Greenland. Polish Polar Res. 38:265–289. DOI:10.1515/popore-2017-0018.

Kalińska-Nartiša E, Lamsters K, Karušs J, Krievāns M, Rečs A, Meija R. 2017b. Fine-grained quartz from cryoconite holes of the Russell Glacier, southwest Greenland – A scanning electron microscopy study. Baltica 30:63–73 DOI:10.5200/baltica.2017.30.08.

Kalińska-Nartiša E, Dzierżek J, Bińka K, Borkowski A, Rydelek P, Zawrzykraj P. 2016a. Upper Pleistocene palaeoenvironmental changes at the Zwierzyniec site, central Poland. Geol. Quat. 60(3):610–623. DOI:10.7306/gq.1280

Kalińska-Nartiša E, Thiel C, Nartišs M, Buylaert J-P, Murray AS. 2016b. The north-eastern aeolian 'European Sand Belt' as potential record of environmental changes: a case study from Eastern Latvia and Southern Estonia. Aeolian Res. 22:59–72. DOI:10.1016/j/aeolia.2016.06.002.

Kalińska-Nartiša E, Thiel C, Nartišs M, Buylaert J-P, Murray AS. 2015. Age and sedimentary record of inland eolian sediments in Lithuania, NE European Sand Belt. Quat Res. (United States) 84:82–95 doi:10.1016/j.yqres.2015.04.001.

Kalm, V, Raukas A, Rattas M, Lasberg K. 2011. Pleistocene Glaciations in Estonia. In: Ehlers, J., Gibbard, P.L., Hughes, P.D. (Eds.), Quaternary Glaciations - Extent and Chronology, Developments in Quaternary Science. Elsevier Inc., Amsterdam:95–104. DOI:10.1016/B978-0-444-53447-7.00008-8.

Kalniņa L, Ceriņa A, Ozola I, Apsite, I. 2011. Palaeobotanical records from the deposits of the Raunis site. In: Lukševics, E., Sinkulis, Ģ., Vasilikova, J. (Eds.), The Eight Baltic Stratigraphical Conference 28 August –1 September 2011, Latvia:32.

Kar R, Mazumder A, Mishra K, Patil SK, Ravindra R, Ranhotra PS, Govil P, Bajpai R, Singh K. 2018. Climatic history of Ny-Alesund region, Svalbard, over the last 19,000 yr_ Insights from quartz grain microtexture and magnetic susceptibility. Polar Sci. 18:189–196.DOI:10.1016/j.polar.2018.04.004.

Kenzler M, Tsukamoto S, Meng S, Frechen M, Hüneke H. 2016. New age constraints from the SW Baltic Sea area - implications for Scandinavian Ice Sheet dynamics and palaeo-environmental conditions during MIS 3 and early MIS 2. Boreas 46(1):34–52. DOI:10.1111/bor.12206.

Koff T, Terasmaa J. 2011. The sedimentary sequence from the Lake Ķūži outcrop, central Latvia: Implications for late glacial stratigraphy. Est J Earth Sci. 60:113–122. DOI:10.3176/earth.2011.2.05.

Lamsters K, Kalińska-Nartiša E, Zelčs V, Alexanderson H. 2017. New luminescence ages reveal early to Middle Weichselian deposits in central Latvia. Geol Q. 61:480–490. DOI:10.7306/gq.1349.

Lowe JJ, Rasmussen SO, Björck S, Hoek WZ, Steffensen JP, Walker MJC, Yu ZC, INTIMATE group, 2008. Synchronisation of palaeoenvironmental events in the North Atlantic region during the Last Termination: a revised protocol recommended by the INTIMATE group. Quat Sci Rev. 27:6–17. DOI:10.1016/j.quascirev.2007.09.016.

Lunkka JP, Sarala P, Gibbard PL. 2015. The Rautuvaara section, western Finnish Lapland, revisited - new age constraints indicate a complex Scandinavian Ice Sheet history in northern Fennoscandia during the Weichselian Stage. Boreas 44:68–80. DOI:10.1111/bor.12088.

Mahaney WC. 2015. Pedological Iron/Al extracts, clast analysis, and coleoptera from antarctic paleosol 831: Evidence of a middle miocene or earlier climatic optimum. J Geol. 123:113–132. DOI:10.1086/680339.

Mahaney WC. 2002. Atlas of sand grain surface, textures and applications. Oxford University Press, Oxford.

Mahaney WC, Claridge G, Campbell I. 1996. Microtextures on quartz grains in tills from Antarctica. Palaeogeogr Palaeoclimatol Palaeoecol 121:89–103.

Mahaney WC, Dirszowsky RW, Milner MW, Menzies J, Stewart A, Kalm V, Bezada M. 2004.

Quartz microtextures and microstructures owing to deformation of glaciolacustrine sediments in the northern Venezuelan Andes. J Quat Sci. 19:23–33. DOI:10.1002/jqs.818.

Major C, Ryan W, Lericolais G, Hajdas I. 2002. Constraints on Black Sea outflow to the Sea of Marmara during the last glacial-interglacial transition. Mar Geol. 190:19–34.

Margolis SV, Krinsley DH. 1971. Submicroscopic Frosting on Eolian and Subaqueous Quartz Sand Grains:3395–3406.

Mazumder A, Govil P, Kar R, Gayathri NM, Raghuram. 2017. Paleoenvironments of a proglacial lake in Schirmacher Oasis, East Antarctica: Insights from quartz grain microtextures. Polish Polar Res. 38:1–19. DOI:10.1515/popore-2017-0002.

Miall AD. 1985. Architectural-element analysis: a new method of facies analysis applied to fluvial deposits. Earth-Sci Rev, 22(4): 261–308. DOI:10.1016/0012-8252(85)90001-7.

Möller P, Murray AS. 2015. Drumlinised glaciofluvial and glaciolacustrine sediments on the Småland peneplain, South Sweden - new information on the growth and decay history of the Fennoscandian Ice Sheets during MIS 3. Quat Sci Rev. 122:1–29. DOI:10.1016/j.quascirev.2015.04.025.

Murray AS, Marten R, Johnson A, Martin P. 1987. Analysis for naturally occuring radionuclides at environmental concentrations by gamma spectrometry. J of Radioanal and Nuch Chem. 115(2):263–288.

Murray AS, Wintle A. 2000. Luminescence dating of quartz using an improved single-aliquot regenerative-dose protocol. Radiat Meas. 32(1):57–73.

Murray AS, Wintle A. 2003. The single aliquot regenerative dose protocol: potential for improvements in reliability. Radiat Meas. 37(4-5):377–381. DOI:10.1016/S1350-4487(03)00053-2.

Oglu Aleskerov BD, Oglu Veliyev SS, Tagiyeva EN. 2010. Climate and change of the Caspian Sea

level during the late 10,000 years. In: Proceedings of the International Conference "The Caspian Region: Environmental Consequences of the Climate Change". October, 14-16. Faculty of Geography Moscow State University, Moscow:64–66.

Pirrus R, Raukas A. 1996. Late-Glacial stratigraphy in Estonia. Proc of the Est Acad Sci Geol. 45:34–45.

Phantuwongraj S, Choowong M, Nanayama F, Hisada, K-I, Charusiri P, Chutakositkanon V, Pailoplee S, Chabangbon A. 2013. Coastal geomorphic conditions and styles of storm surge washover deposits from Southern Thailand. Geomorph. 192:43–58: DOI:10.1016/j.geomorph.2013.03.016

Poska A, Saarse L. 2002. Biostratigraphy and 14C dating of a lake sediment sequence on the north-west Estonian carbonaceous plateau, interpreted in terms of human impact in the surroundings. Veg. Hist. Archaeobot. 11:191–200. DOI:10.1007/s003340200022.

Potapova O. 2001. Snowy owl *Nyctea scandiaca* (Aves: Strigiformes) in the Pleistocene of the Ural Mountains with notes on its ecology and distribution in the Northern Palearctic. DEINSEA 8:103–126.

Punning JM, Liiva A, Ilves E. 1968. Tartu radiocarbon dates III. Radiocarbon 10:379–383.

Ramsey B. 2017. OXCAL-4.3. 2: https://c14. arch. ox. ac. uk/oxcal.

Rasmussen SO, Bigler M, Blockley SP, Blunier T, Buchardt SL, Clausen HB, Cvijanovic I, Dahl-Jensen D, Johnsen SJ, Fischer H, Gkinis V, Guillevic M, Hoek WZ, Lowe JJ, Pedro JB, Popp T, Seierstad IK, Steffensen JP, Svensson AM, Vallelonga P, Vinther BM, Walker MJC, Wheatley JJ, Winstrup M. 2014. A stratigraphic framework for abrupt climatic changes during the Last Glacial period based on three synchronized Greenland ice-core records: Refining and extending the INTIMATE event stratigraphy. Quat Sci Rev. 106:14–28. DOI:10.1016/j.quascirev.2014.09.007.

Raukas A. 2009. When and how did the continental ice retreat from Estonia? Quat Int. 207:50–57. DOI:10.1016/j.quaint.2008.11.010.

Raukas A, Stankowski W, Zelčs V, Šinkunas P. 2010. Chronology of the Last Deglaciation in the Southeastern Baltic Region on the Basis of Recent OSL Dates. Geochronometria 36: 47–54. DOI:10.2478/v10003-010-0011-7.

Rinterknecht VR, Clark PU, Raisbeck GM, Yiou F, Bitinas A, Brook EJ, Marks L, Zelcs V, Lunkka J-P, Pavlovskaya IE, Piotrowski JA, Raukas A. 2006. The last deglaciation of the southeastern sector of the Scandinavian ice sheet. Science 311:1449–52. DOI:10.1126/science.1120702.

Rivals F, Kitagawa K, Julien M-A, Bessudnov AA, Bessudnov AN. 2018. Straight from the horse's mouth: High resolution proxies for the study of horse diet and its relation to the seasonal occupation patterns at Divnogor'ye 9 (Middle Don, Central Russia). Quat Int. 474:146–155. DOI:10.1016/j.quaint.2018.01.008.

Savvaitov AS, Stelle V, Krukle M. 1964. On stratigraphic subdivision of deposits of the Valdaian glaciation in the territory of the Latvian SSR. In: Danilans IJ. (Ed.), Questions of Quaternary Geology, II. Zinātne, Riga:183–201. Russian

Savvaitov AS, Straume J. 1963. On the problem of two till units of the Valdaian Glaciation in the area between the lower reaches of the Rivers Daugava and Gauja. In: Danilān I. (Ed.), Questions of Quaternary Geology, 2. Zinātne, Riga:71–86. Russian

Stelle V, Savvaitov AS, Jakubovska I. 1999. Complex of deposits on the bank of the Raunis River, its structure and age. In: Klavinš M. (Ed.), Zeme Daba Cilveks, LU 57. Konferences Geografijas, Geologijas Un Vides Zinatnu Sekcija. University of Latvia, Riga:130–132. Latvian.

Stelle V, Savvaitov AS, Veksler VS. 1975a. Absolute age of chronostratigraphical stages and boundaries of late-glacial and postglacial in the territory of central Baltic. In: Afanasyev GD. (Ed.), Sostoyaniye Metodicheskikh Issledovaniy v Oblasti Absolyutnoy Geokhronologii.

Nauka, Moscow:187–191. Russian.

Stelle V, Savvaitov AS, Veksler VS. 1975b. Dating of Pleistocene deposits in the territory of Latvia. In: Savvaitov AS, Veksler VS. (Eds.), Opyt i Metodika Izotopno-Geokhimicheskikh Issledovaniy v Pribaltike i Belorussii:80–81. Russian.

Stivrins N, Brown A, Veski S, Ratniece V, Heinsalu A, Austin J, Liiv M, Ceriņa A. 2016. Palaeoenvironmental evidence for the impact of the crusades on the local and regional environment of medieval (13th–16th century) northern Latvia, eastern Baltic. The Holocene 26:61–69. DOI:10.1177/0959683615596821.

Stroeven AP, Hättestrand C, Kleman J, Heyman J, Fabel D, Fredin O, Goodfellow BW, Harbor JM, Jansen JD, Olsen L, Caffee MW, Fink D, Lundqvist J, Rosqvist GC, Strömberg B, Jansson KN. 2016. Deglaciation of Fennoscandia. Quat Sci Rev. 147:91–121. DOI:10.1016/j.quascirev.2015.09.016.

Svendsen JI, Alexanderson H, Astakhov VI, Demidov I, Dowdeswell JA, Funder S, Gataullin V, Henriksen M, Hjort C, Houmark-Nielsen M, Hubberten HW, Ingólfsson Ó, Jakobsson M, Kjær KH, Larsen E, Lokrantz H, Lunkka JP, Lyså A, Mangerud J, Matiouchkov A, Murray A, Möller P, Niessen F, Nikolskaya O, Polyak L, Saarnisto M, Siegert C, Siegert MJ, Spielhagen RF, Stein R. 2004. Late Quaternary ice sheet history of northern Eurasia. Quat Sci Rev. 23:1229–1271. DOI:10.1016/j.quascirev.2003.12.008.

Sycheva SA, Bessudnov AN, Chepalyga AL, Sadchikova TA, Sedov SN, Simakova AN, Bessudnov AA. 2016. Divnogorie pedolithocomplex of the Russian Plain: Latest Pleistocene deposits and environments based on study of the Divnogorie 9 geoarchaeological site (middle reaches of the Don River). Quat Int. 418:49–60. DOI:10.1016/j.quaint.2015.11.006.

Timar-Gabor A, Vandenberghe D, Panaiotu EC, Panaiotu CG, Necula C, Cosma C,Van den haute P. 2010. Optical dating of Romanian loess using fine-grained quartz. Quat Geochr 5:143–148. DOI:10.1016/j.quageo.2009.03.003

Vandenberghe J, Sidorchuk A. 2020. Large palaeomeanders in Europe: distribution, formation process, age, environments and significance. In: Palaeogydrology, Springer, Cham:169–186.

Van der Hammen T, Vogel JC. 1966. The Susaca-Interstadial and the subdivision of the Late Glacial. Geol en Mijnbouw/Netherlands J Geosci. 45:33–35.

van Hoesel A, Hoek WZ, Pennock GM, Drury MR. 2014. The Younger Dryas impact hypothesis: a critical review. Quat Sci Rev. 83:95–114. DOI:10.1016/j.quascirev.2013.10.033.

Veski S, Amon L, Heinsalu A, Reitalu T, Saarse L, Stivrins N, Vassiljev J. 2012. Lateglacial vegetation dynamics in the eastern Baltic region between 14,500 and 11,400calyrBP: A complete record since the Bølling (GI-1e) to the Holocene. Quat Sci Rev. 40:39–53. DOI:10.1016/j.quascirev.2012.02.013.

Vinogradov AP, Devirts AL, Dobkina EI, Markova NG. 1963. Determination of the absolute age according to C14. Geochemistry 9:795–812.

Vos K, Vandenberghe N, Elsen J. 2014. Surface textural analysis of quartz grains by scanning electron microscopy (SEM): From sample preparation to environmental interpretation. Earth-Science Rev. 128:93–104. DOI:10.1016/j.earscirev.2013.10.013.

Weckwerth P, Przegiętka KR, Chruścińska A, Pisarska-Jamroży M. 2012. The relation between optical bleaching and sedimentological features of fluvial deposits in the Toruń Basin (Poland). Geol Q. 56:31–44. DOI:10.7306/gq.1074.

Weckwerth P, 2018. Fluvial responses to the Weichselian ice sheet advances and retreats: implications for understanding river paleohydrology and pattern changes in Central Poland. Int J of Earth Sc. 107: 1407–1429. DOI:10.1007/s00531-017-15450-y

Widdowson M. 1997. Palaeosurfaces: recognition, reconstruction and palaeoenvironmental interpretation. Geological Society, London.

Woronko B, 2012. Micromorphology of quartz grains as a tool in the reconstruction of periglacial

environment. In: Churski P. (Ed.), Contemporary Issues in Polish Geography. Bogucki Wydawnictwo Naukowe, Poznań:111–131. Polish.

Zelčs V, Markots A, 2004. Deglaciation history of Latvia. In: Ehlers J, Gibbard PL (Eds.), Quaternary Glaciations Extent and Chronology Part I: Europe, Developments in Quaternary Science. Elsevier, Amsterdam:225–243. DOI:http://dx.doi.org/10.1016/S1571-0866(04)80074-5.

Zelčs V, Markots A, Nartišs M, Saks T. 2011. Pleistocene Glaciations in Latvia, in: Ehlers, J., Gibbard, P.L., Hughes, P.D. (Eds.), Quaternary Glaciations - Extent and Chronology, Developments in Quaternary Science. Elsevier, Amsterdam:221–229. DOI:10.1016/B978-0-444-53447-7.00018-0.

Zelčs V, Nartišs M, 2014. Outlines of the Quaternary geology of Latvia, Excursion guide and abstracts of the INQUA Peribaltic Working Group Meeting and field excursion in Eastern and Central Latvia, August 17-22, 2014. University of Latvia.

Zhang JF, Zhou LP, Yue SY, 2003. Dating fluvial sediments by optically stimulated luminescence: selection of equivalent doses for age calculation. Quat Sci Rev. 22(10–13):1123–1129. DOI:10.1016/S0277-3791(03)00054-4.

Zobens V, Putans B, Stelle V. 1969. The first dating of absolute age in the Riga radiocarbon laboratory. In: Danilans IJ. (Ed.), Problems of Quaternary Geology IV. Zinātne, Riga:141–145.

Table 1. Details about sampling at Raunis.

Sample no.	Laboratory no.	Unit
R1	Lund-16001	2
AMS	LuS 13695	2
R2	Lund-16002	2
R3	no sample	3a
R4	Lund-16003	3a
R5	Lund-16004	3a
R6	Lund-16005	3a
R7	Lund-16006	3b
R8	Lund-16007	3b
R9	Lund-16008	1

Table 2. Obtained ^{14}C AMS age of the Raunis compared to previously published ages.

Lab code	Uncalibrated dates (BP)	Calibrated (Oxcal 4.3) dates (cal BP) from to:	Calibrated (Oxcal 4.3) dates (cal BP)	references
Mo-296	13,390±500	17637-14534	16,086±1552	Vinogradov et al. (1963)
Ta-177	13,250±160	16355-15369	15,862±493	Punning et al (1968)
Ri-39	13,320±250	16777-15271	16,024±753	Stelle et al. (1975 a, b)
Ri-5	10,780±220	13106-12089	12,598±509	Zobens et al. (1969)
Ri-5A	10,400±370	13043-11189	12,116±927	Zobens et al. (1969)
no data	8,020±70	9034-8639	8,837±198	Zelčs and Markots (2004)
Tln-2319	9,302±83	10695-10261	10,478±217	Raukas (2009)
Tln-2322	9,227±70	10556-10245	10,401±156	Raukas (2009)
Poz-38330	11,350±70	13324-13070	13,197±127	Amon (2011), unpublished data
Poz-38331	11,420±60	13405-13126	13,266±140	Amon (2011), unpublished data
LUS 13695	12,150±90	14295-13755	14,025±270	this study

Table. 3. OSL data with Central Age Model (CAM) and Minimum Age Model (3 parameters, MAM3) ages. Preferred ages in bold. 'n' is number of accepted and measured aliquots, 'w.c.' is water content ± 4% of uncertainty. The low number of aliquots for some samples is mainly due to a high apparent feldspar contamination, which for some samples had a correlation with dose, and to poor recycling ratios.

Sample no.	Lab no. Lund-	Depth (cm)	Unit	CAM age (ka)	MAM3 age (ka)	p	Mean dose (Gy)	n	Overdiscperion (OD)	Skewness	Dose rate (Gy/ ka)	w.c. (%)
R1	16001	330	2	**12.0 ± 0.6**	-	-	32.6 ± 1.5	21/42	16 ± 3.4	0.12	2.696 ± 0.083	48
R2	16002	310	2	123 ± 12	**121.6 ± 8.6**	1.0	208 ± 16	31/44	40 ± 6	0.62	1.494 ± 0.095	21
R4	16003	280	3a	48.1 ± 7.3	**34.1 ± 5.4**	0.12	91.5±7.8	26/38	41 ± 6	0.99	1.720 ± 0.218	21
R5	16004	248	3a	**49.3 ± 3.8**	-	-	136.8 ± 8.6	36/57	39 ± 5.1	0.33	2.537 ± 0.097	22
R6	16005	232	3a	**36.5 ± 3.2**	17.8 ± 1.9	0.005	83.3 ± 7.7	24/33	36 ± 5.8	1.5	2.037 ± 0.080	25
R7	16006	165	3b	**30.3 ± 4.0**	8.8 ± 2.0	0.008	73.4 ± 9.4	20/24	55 ± 9.2	1.35	2.033 ± 0.077	25
R8	16007	190	3b	**27.0 ± 2.4**	-	-	47 ± 2.9	21/48	27 ± 4.7	0.35	1.669 ± 0.109	29
R9	16008	400	1	**59.2 ± 6.9**	-	-	115 ± 12	23/33	49 ± 7.6	0.5	1.739 ± 0.091	17

Figure 1

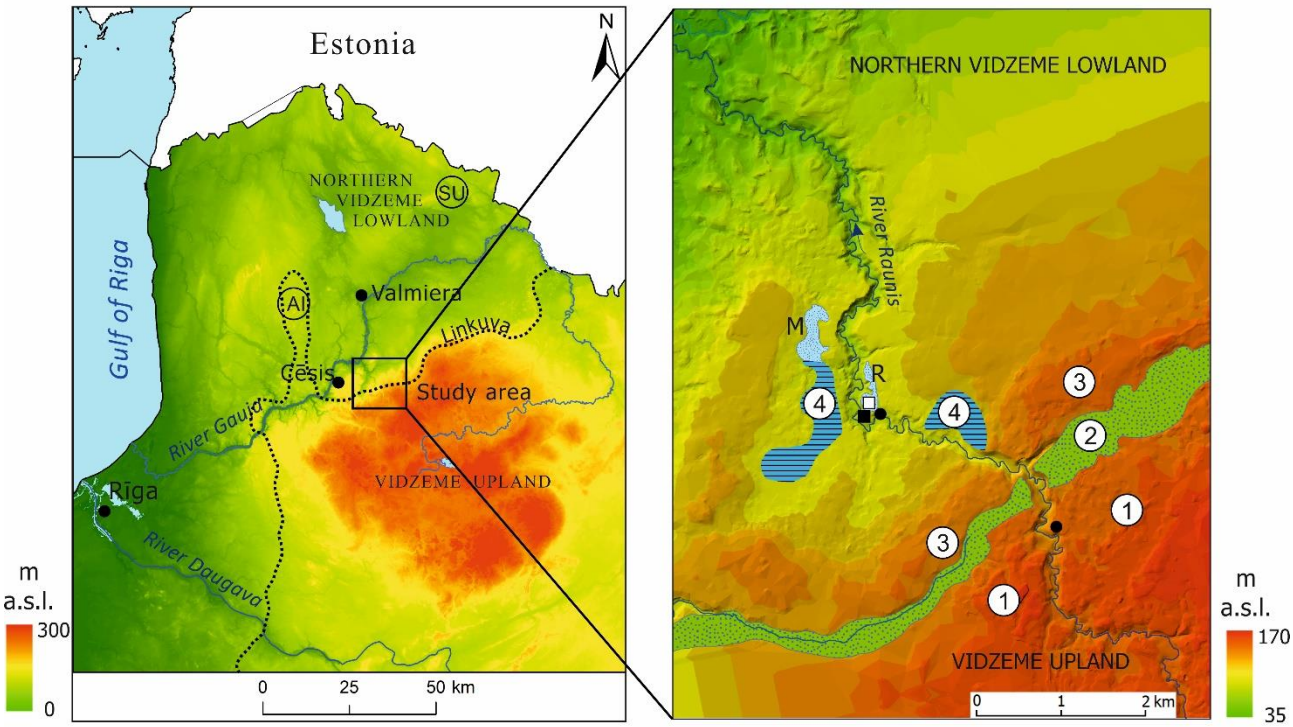
Estonia
N
NORTHERN VIDZEME LOWLAND
SU
Gulf of Riga
Valmiera
AI
Linkuva
Cēsis
Study area
River Gauja
VIDZEME UPLAND
Rīga
River Daugava
m a.s.l.
300
0
0 25 50 km
NORTHERN VIDZEME LOWLAND
River Raunis
M
R
4
4
3
2
1
3
1
VIDZEME UPLAND
0 1 2 km
m a.s.l.
170
35

860

Figure 2

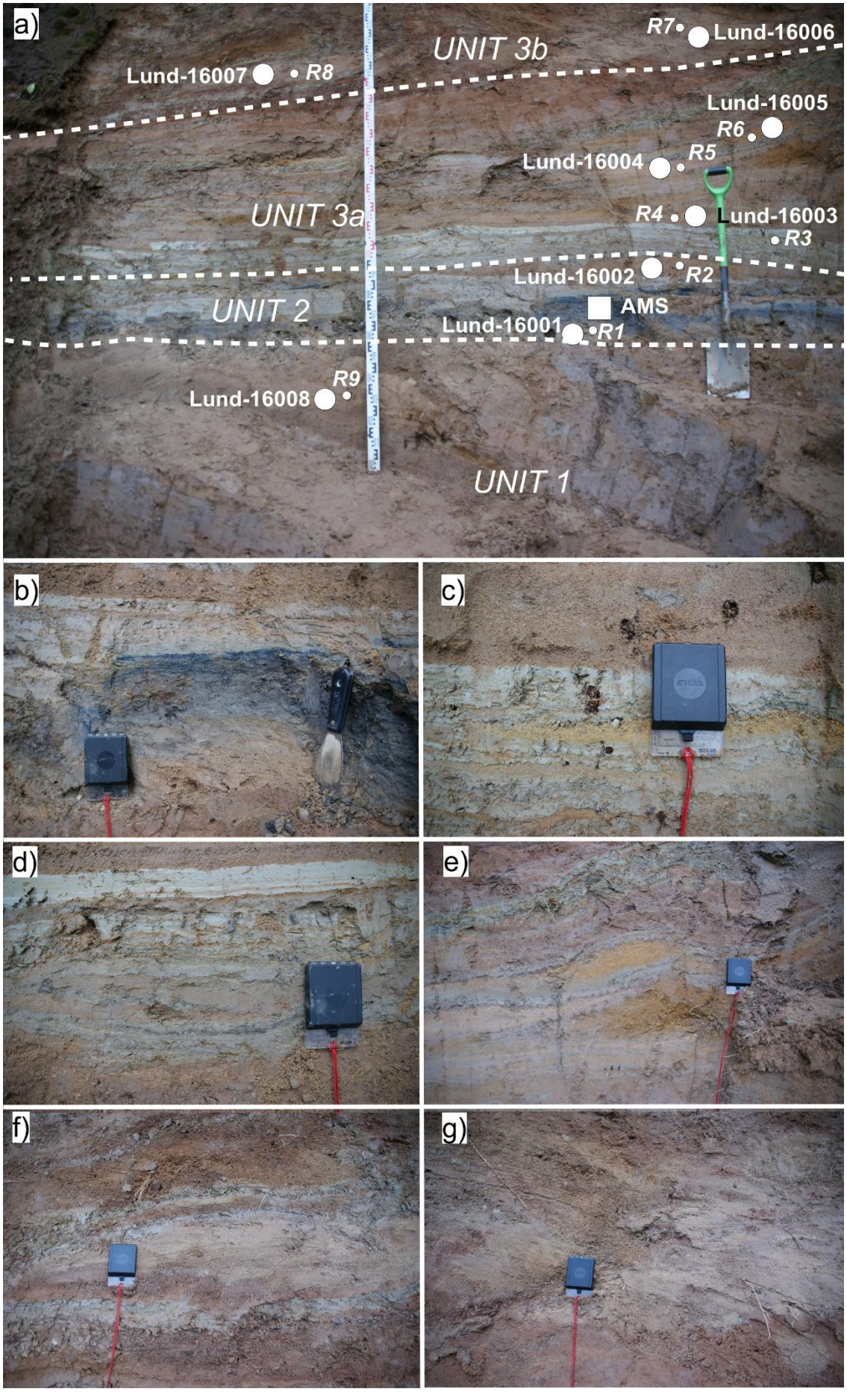
a)
UNIT 3b
UNIT 3a
UNIT 2
UNIT 1
Lund-16007
R8
R7
Lund-16006
Lund-16005
R6
Lund-16004
R5
R4
Lund-16003
R3
Lund-16002
R2
AMS
Lund-16001
R1
R9
Lund-16008
b)
c)
d)
e)
f)
g)

Figure 3

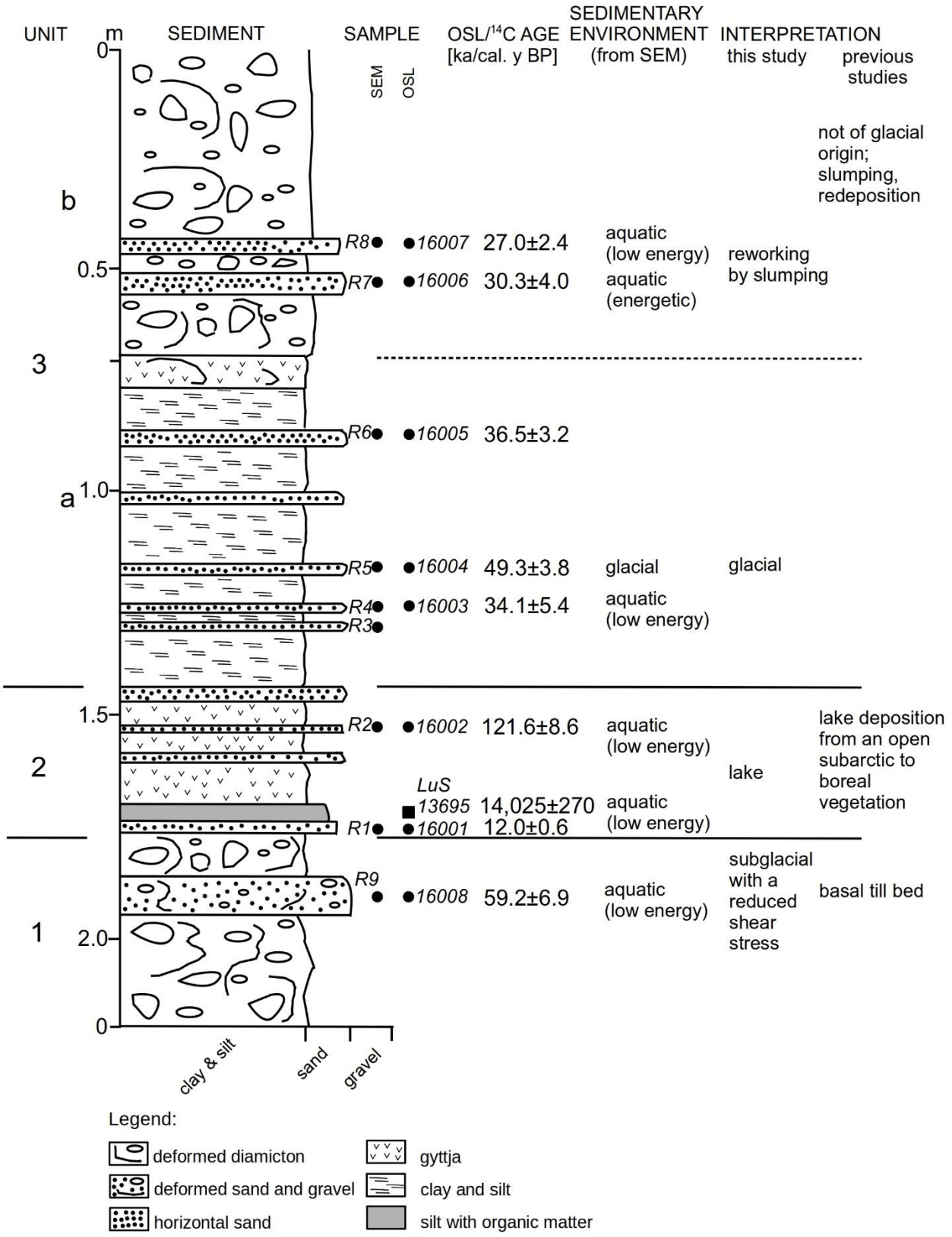
UNIT
m
SEDIMENT
SAMPLE
SEM
OSL
OSL/14C AGE [ka/cal. y BP]
SEDIMENTARY ENVIRONMENT (from SEM)
INTERPRETATION
this study
previous studies
not of glacial origin; slumping, redeposition
b
R8
16007
27.0±2.4
aquatic (low energy)
reworking by slumping
0.5
R7
16006
30.3±4.0
aquatic (energetic)
3
R6
16005
36.5±3.2
a
1.0
R5
16004
49.3±3.8
glacial
glacial
R4
16003
34.1±5.4
aquatic (low energy)
R3
1.5
R2
16002
121.6±8.6
aquatic (low energy)
lake deposition from an open subarctic to boreal vegetation
2
LuS
13695
14,025±270
aquatic (low energy)
lake
R1
16001
12.0±0.6
subglacial with a reduced shear stress
R9
16008
59.2±6.9
aquatic (low energy)
basal till bed
1
2.0
0
clay & silt
sand
gravel
Legend:
deformed diamicton
deformed sand and gravel
horizontal sand
gyttja
clay and silt
silt with organic matter

865

Figure 4

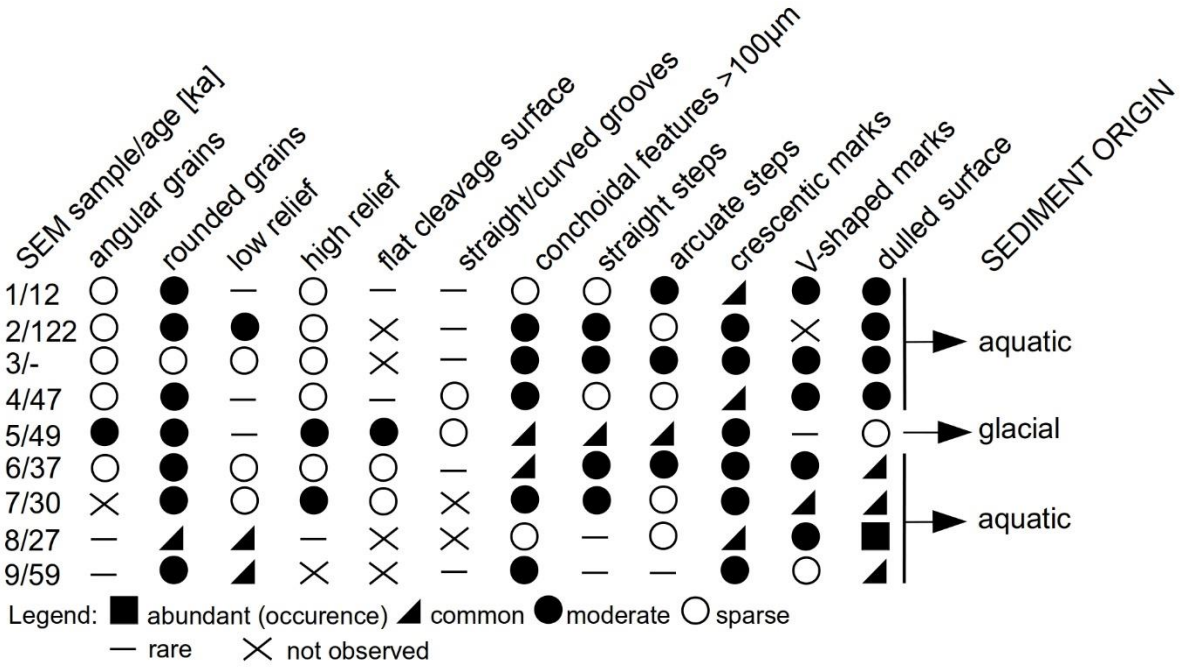
SEM sample/age [ka]
angular grains
rounded grains
low relief
high relief
flat cleavage surface
straight/curved grooves
conchoidal features >100µm
straight steps
arcuate steps
crescentic marks
V-shaped marks
dulled surface
SEDIMENT ORIGIN
1/12
2/122
3/-
4/47
5/49
6/37
7/30
8/27
9/59
aquatic
glacial
aquatic
Legend: abundant (occurence) common moderate sparse
rare
not observed

870 Figure 5

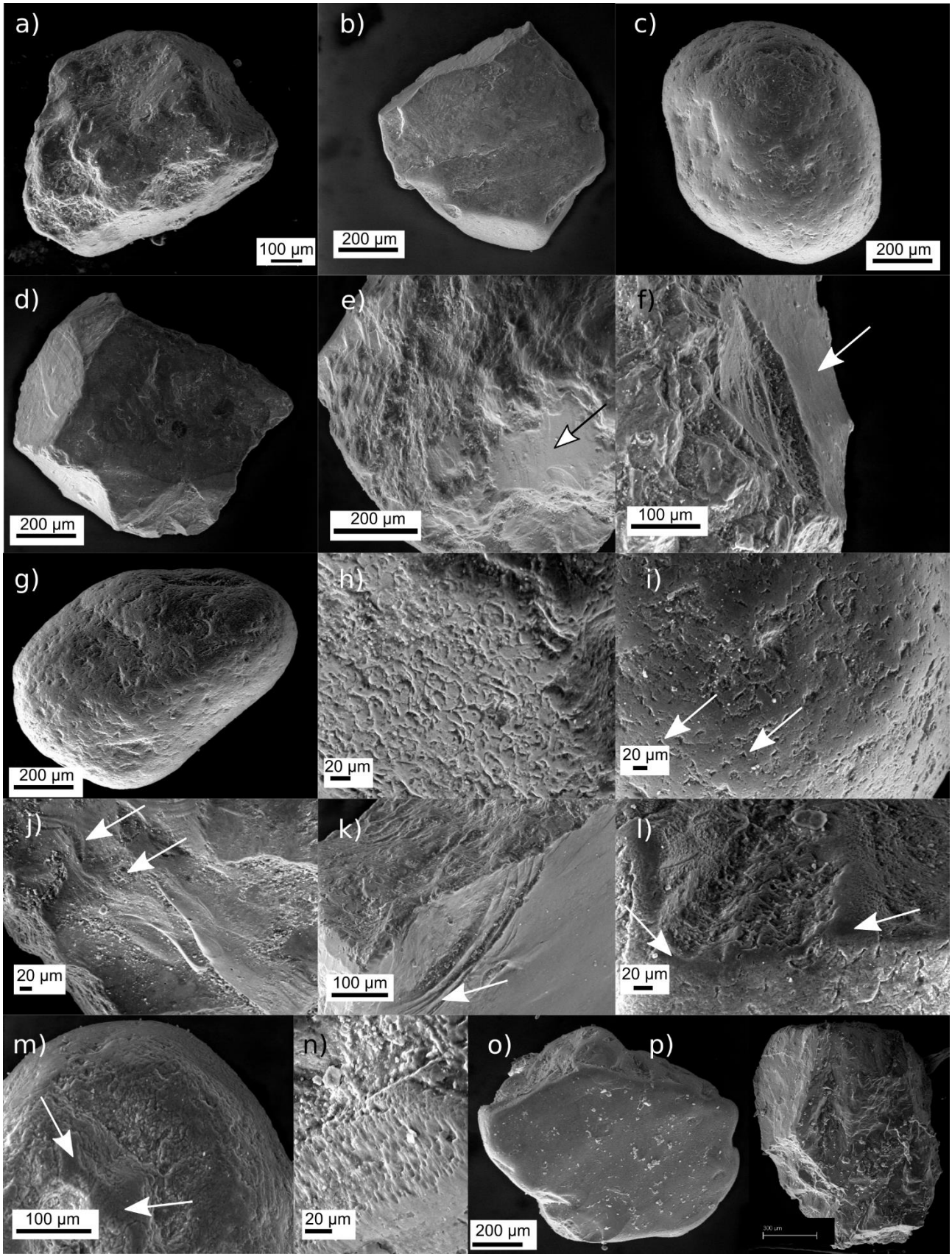
a)
100 µm
b)
200 µm
c)
200 µm
d)
200 µm
e)
200 µm
f)
100 µm
g)
200 µm
h)
20 µm
i)
20 µm
j)
20 µm
k)
100 µm
l)
20 µm
m)
100 µm
n)
20 µm
o)
200 µm
p)

Figure 6

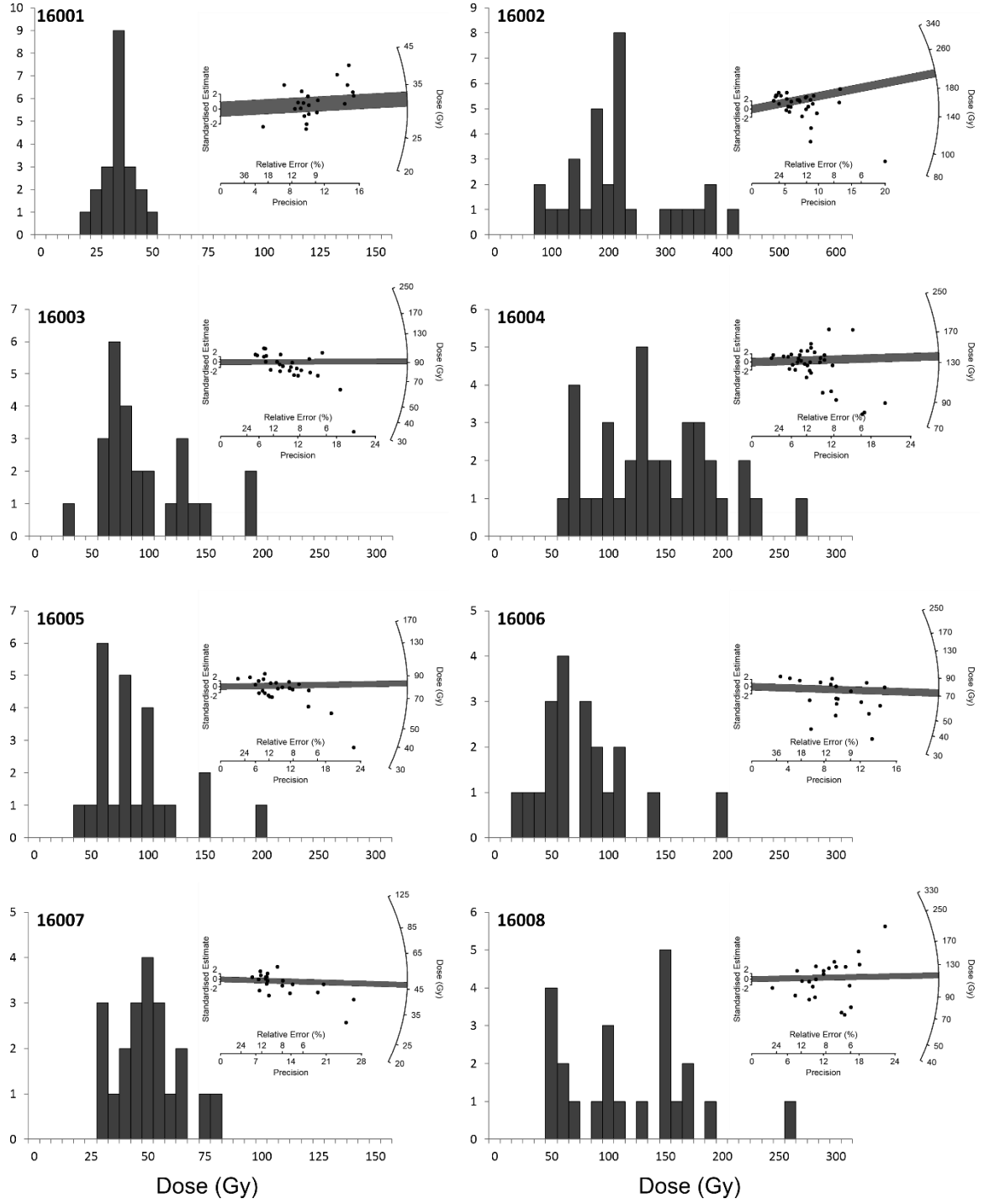
16001
16002
16003
16004
16005
16006
16007
16008
Standardised Estimate
Relative Error (%)
Precision
Dose (Gy)
Dose (Gy)

875

Figure 7